Collection de notes internes
de la Direction
des Etudes et Recherches

Production d'énergie (hydraulique, thermique et nucléaire)

COMPORTEMENT THERMOMECANIQUE ET MODELISATION DES GAINES EN ZIRCALOY SANS ET SOUS FORTE IRRADIATION

THERMOMECHANICAL BEHAVIOR AND MODELING OF ZIRCALOY CLADDING TUBES FROM AN UNIRRADIATED STATE TO HIGH BURN-UP

97NB00102

EDF
Electricité de France

DIRECTION DES ÉTUDES ET RECHERCHES

SERVICE RÉACTEURS NUCLÉAIRES ET ECHANGEURS
DÉPARTEMENT MÉCANIQUE ET TECHNOLOGIE DES COMPOSANTS

EDF
Electricité de France

1997

SCHAFFLER-LE PICHON I.
GEYER P.
BOUFFIOUX P.
DELOBELLE P.

COMPORTEMENT THERMOMECANIQUE ET MODELISATION DES GAINES EN ZIRCALOY SANS ET SOUS FORTE IRRADIATION

THERMOMECHANICAL BEHAVIOR AND MODELING OF ZIRCALOY CLADDING TUBES FROM AN UNIRRADIATED STATE TO HIGH BURN-UP

Pages : 12

97NB00102

Diffusion : J.-M. Lecœuvre
EDF-DER
Service IPN. Département PROVAL
1, avenue du Général-de-Gaulle
92141 Clamart Cedex

ISSN 1161-0611

SYNTHÈSE :

Les lois de fluage sont utilisées couramment pour simuler la réponse du crayon combustible (pastille et gaine) aux sollicitations qu'il rencontre au cours de sa vie. De telles lois sont suffisantes pour décrire les conditions de fonctionnement en base (où seuls les mécanismes de fluage sont activés), mais elles doivent être améliorées pour décrire correctement les conditions de rampes de puissance (où des phénomènes d'écrouissage et de relaxation apparaissent).

Dans un premier temps, la note met en évidence les modifications induites par l'irradiation sur le comportement thermomécanique du Zircaloy-4 détendu. A cet effet, cinq fluences sont examinées, depuis le matériau non-irradié, jusqu'à des taux de combustion élevés.

Dans une deuxième partie, un modèle de comportement viscoplastique est proposé. Ce modèle permet de simuler le comportement mécanique anisotrope de la gaine à différents taux de combustion, et pour différentes isothermes.

Les comparaisons entre simulations numériques et essais expérimentaux montrent la capacité prédictive du modèle.

EXECUTIVE SUMMARY :

Creep laws are nowadays commonly used to simulate the fuel rod response to the sollicitations it faces during its life. These laws are sufficient for describing the base operating conditions (where only creep appears), but they have to be improved for power ramp conditions (where hardening and relaxation appear).

~~This paper first introduces~~ The modification due to a neutronic irradiation of the thermomechanical behavior of stress-relieved Zircaloy 4 fuel tubes that have been analysed for five different fluences ranging from a non-irradiated material to a material for which the combustion rate was very high ~~is~~ is presented.

In the second part, ~~it is proposed~~ a viscoplastic model able to simulate, for different isotherms, out-of-flux anisotropic mechanical behavior of the cladding tubes irradiated until high burn-up is proposed

Finally, results of numerical simulations show the ability of the model to reproduce the totality of the thermomechanical experiments.

Thermomechanical behavior and modeling of Zircaloy cladding tubes from an unirradiated state to high burn-up

I. Schäffler-Le Pichon*, P. Geyer*, P. Bouffioux* and P. Delobelle**

* Electricité de France, Direction des Etudes et Recherches,
Dpt. MTC, Route de Sens, 77250 MORET/LOING, France

** Laboratoire de Mécanique Appliquée R. Chaléat, URA CNRS 04,
24 rue de l'Epitaphe, 25030 BESANCON CEDEX, France

I - INTRODUCTION

Today, over 70 % of the French electric power has a nuclear origin and is generated by 58 PWR pressurized water units. This capacity makes it necessary for reactors to adapt their production rate to the network demand by operating under load follow-up conditions. Moreover, due to economic reasons, Electricity of France wants to extend the fuel assembly life span so as to ultimately reach a 60 GWd/tU (Giga-Watt-day/ton Uranium) mass depletion rate. These new conditions of use bring about more severe mechanical loadings of the cladding than initially provided due to a greater increase of the number of power ramps.

Behavior laws currently used for predicting the mechanical behavior of fuel rod claddings do not integrate the whole loading modes inherent in these operating conditions [1]. This requires developing a behavior model capable of more sharply calculating the material anisotropic behavior and more specifically, the stress relaxation in cladding following a loading with a pellet-cladding interaction (PCI) resulting from a power ramp. Such a model should also be fit for taking into account irradiation effects upon the mechanical properties at high-rate fluences which may reach 100.10^{24} nm^{-2} ($E > 1$ MeV) and at temperatures ranging from 350 to 400°C, which is the cladding operating temperature range. Deformations are conventionally dealt with as deformations linked to the material growth, deformations occuring under irradiation flux and deformations called "thermal" which are due to power transients. Thermal deformations are chosen for the simulation of cladding behavior resulting form PCI [1].

EDF has launched, in collaboration with some industrial partners, new testing programs on stress-relieved Zircaloy-4 cladding tubes of the same type as those used in PWR power plants. This new data base is now available and has allowed us to develop a behavior model which takes into account the anisotropy, the temperature and the irradiation effects upon the cladding

mechanical properties. The data base includes monotonic tension and uni-axial creep tests, bi-axial loading tension tests followed by a relaxation phase, and bi-axial creep tests.

II - TESTED MATERIALS AND EXPERIMENTAL RESULTS

II.1 Tested materials

Mechanical tests have been carried out on CWSR cladding tubes with nominal dimensions 9.5 mm outside diameter and 0.57 mm wall thickness. The chemical composition of these tubes is given in Table 1. The content of alloying elements is consistent with the ASTM B 353 specification.

Table 1 - Weight composition of Zircaloy-4

Alloying elements (%)					Impurities (ppm)		
Cr : 0.10	Fe : 0.21	Sn : 1.25	0 : 0.11	Zr : bal.	C : 120	N : 31	H < 2

The texture analysis reveals a fairly pronounced anisotropy. The Kearns factors show the radial trend for the crystallographic texture : $f_r = 0.57$, $f_a = 0.35$ and $f_z = 0.08$, in radial, tangential and longitudinal directions respectively. By assuming that the texture axis is identical with the anisotropic axis, then the tube has an orthotropic mechanical behavior.

II.2 Mechanical tests realized on unirradiated cladding tubes

Monotonic axial tension tests have been performed at 350 and 400°C for different strain rates between 2.10^{-6} and $2.10^{-3} s^{-1}$. The experimental tests reveal the strong viscosity of the material at these temperatures. The Rp ratio of the plastic hoop strain to the axial one, $R^p = \varepsilon^p_{\theta\theta} / \varepsilon^p_{zz}$, is found to be, as a first approximation, independent of temperature and strain rate. To simplify the description of anisotropy in the model, the set of anisotropy coefficients will be considered as independent of temperature and strain-rate, which corroborates the results of Beauregard and al. [2] and Murty [3].

To characterize the anisotropy of these tubes, biaxial tensile tests are performed for different stress-biaxiality ratio α ($\alpha = \sigma_{\theta\theta}/\sigma_{zz}$, hoop stress divided by the longitudinal stress). These tests are carried out with a machine which allow us to impose the biaxiality ratio α, knowing the hoop stress. An example of curves $\sigma_\theta = f(\varepsilon_\theta)_\alpha$ is given in Fig. 1. Uniaxial ($140 < \sigma_{zz} < 400$ MPa) and biaxial ($100 < \sigma_{\theta\theta} < 175$ MPa) creep tests are also realized.

II.3 Mechanical tests performed out-of-flux on irradiated CWSR cladding tubes

The data base consists of three programs respectively designated by A, B and C. These programs will allow us to quantify the effects of irradiation upon a fuel rod cladding throughout the life span of assemblies up to high burn-up.

- Program A [4]. Test specimens taken from tubes similar to those described earlier are introduced into capsules and irradiated in an experimental reactor. Some test specimens have been removed after 500, 1000 and 3000 hours so as to obtain claddings irradiated at different fluence levels, say about 4.10^{24}, 8.10^{24} and 21.10^{24} n/m^2 (E > 1 MeV). The upper fluence level reached is that of a cladding irradiated during one cycle in a PWR reactor. These samples have undergone no hydration or corrosion and have not been exposed to any mechanical loading.

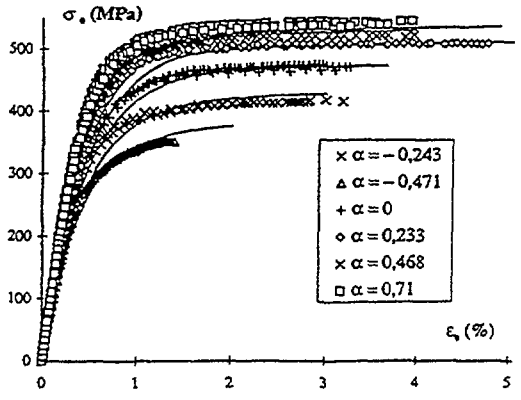

• Fig. 2 : Evolution of the flow stress, for different strains, with the fluence. $\dot{\varepsilon}_\theta = 5.10^{-6} s^{-1}$ and T = 350°C.

• Fig. 1 : Biaxial tensile tests performed at 350°C for different stress-biaxiality ratio $\alpha = \sigma_{\theta\theta}/\sigma_{zz}$.

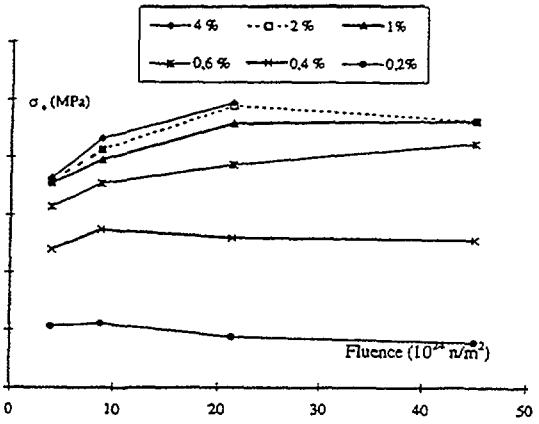

• Fig. 3 : Steady creep strain rates versus the fluence (Programs A,B,C) at 350°C and for different stress levels.

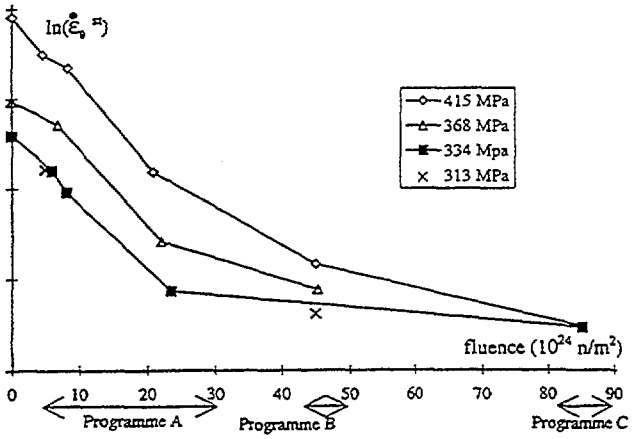

• Fig. 4 : Biaxial tensile test, α = 0.5, with an imposed hoop strain rate $\dot{\varepsilon}_\theta = 2.10^{-5} s^{-1}$ followed by a relaxation test, for T = 350, 380 and 400°C. These loadings are representative of a PCI transient.

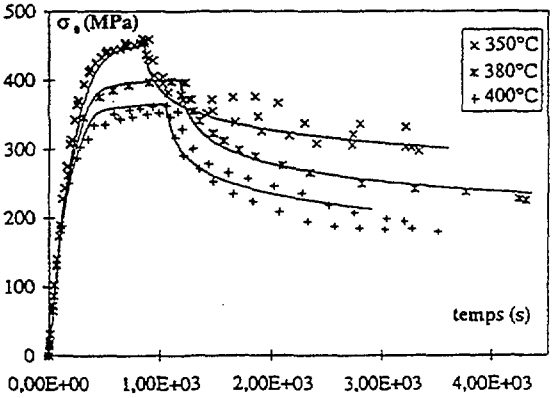

Strain hardening tests under internal pressure (α = 0.5) have then been conducted at two loading rates, say 2.10^{-4} and $5.10^{-6}s^{-1}$ at 350 and 380°C. These tests have been completed by twelve creep tests performed at 350°C and three tests at 380°C.

- Program B [5]. Claddings made of CWSR low-tin content Zircaloy-4 are irradiated in a PWR reactor. These claddings come from fuel rods taken from a single assembly following two operating cycles. Test specimens are cut from the fuel rods and a chemical decladding of the fuel is made. These operations therefore allow us to obtain specimens that have been irradiated up to a fluence of 45.10^{24} n/m^2 (E > 1 MeV). It is worth noting that claddings are corroded and hydrided as they have been in contact with the primary medium. Irradiated test specimens are subject to bi-axial tensile tests (α = 0.5) at three required deformation rates : 2.10^{-4}, 2.10^{-5} and $5.10^{-6}s^{-1}$, and to creep tests for five stress levels ranging from 300 to 520 MPa at 350°C. Other creep tests have also been performed at 380°C.

- Program C [6]. Tests are conducted on test specimens cut from a fuel rod irradiated during four cycles in a PWR reactor. These claddings are consequently corroded and hydrided too. Bi-axial tensile tests (α = 0.5) have been conducted at 350, 380 and 400°C given deformation rates ranging from 1.4 10^{-4} to 1.4 $10^{-7}s^{-1}$. Creep tests have also been realized at these temperatures given tangential stress levels ranging from 300 to 500 MPa.

II.4 Analysis of the results obtained on irradiated claddings

The elastic behavior of the material does not seem to be significantly modified by the neutronic flux. However, the inelastic behavior of the claddings is strongly affected by the irradiation. We have plotted in Fig. 2 the variations of the flow stress required for obtaining a given deformation versus the fluence, at 350°C and at loading rate of $5.10^{-6}s^{-1}$. This graph proves that the irradiation makes the material harden at a high rate at fluences ranging from 10. to 20.10^{24} n/m^2 and that it then tends to become stable. The saturation in the evolution of mechanical properties during tensile tests relative to the fluence confirms the conclusions obtained by several authors [7-8]. During the secondary creep phase, strain hardening could be regarded as being constant and it is therefore possible to analyse the recovery phenomenon by analysing the curves of the diametrical deformation steady rate versus the constant stress for different fluences. From this representation it is possible to obtain the Fig. 3 which shows how the secondary creep rate varies at 350°C as a function of the fluence. We plot on this figure the points derived from tests performed within the framework of programs A, B and C. We see that the creep rate becomes much lower before stabilized for high fluences according to the results given in references [9-11]. Note that the whole results seem therefore consistent (Fig. 2 and 3).

III - MODELING AT DIFFERENT TEMPERATURES OF THE BEHAVIOR OF IRRADIATED ZIRCALOY-4

We worked with a behavior model developed on other types of materials and adapted to the Zircaloy case [12-13]. The equations of the model are given in Table II. By admitting the case of small deformations, the total strain can be splitted into two terms, an elastic strain [ε^e] considered isotropic and a viscoplastic strain [ε] which is anisotropic. Experimental studies including cyclic tests clearly indicated the kinematical nature of the hardening. So, the stress is the sum of two components, a viscous stress $\sigma_v = \overline{\sigma - \alpha}$ and an internal stress [α]. Three kinematical variables are necessary to simulate the strong linearity of the mechanical behavior of Zircaloy. The evolution laws of the kinematical hardening variables [α], [$\alpha^{(1)}$] and [$\alpha^{(2)}$] define the mechanical behavior completely. The first term of these equations is the linear part

of the hardening, the second term represents the dynamic recovery and the last one represents the time dependent static recovery. The introduction of the anisotropy in this model is made via the four fourth rank tensors affecting the flow directions [M], the linear part of kinematical hardening [N], as well the dynamic and static recoveries, [Q] and [R], of these same hardening variable. Y is a scalar variable which describe the hardening of the material during cyclic loadings.

Irradiation causes a marked hardening while reducing the creepability of the material. To take into account the saturation observed in the evolution of the mechanical properties, we do not use the fluence ϕ as a damage variable but a state variable denoted D in table II. A number of model parameters will depend upon this variable. Note that such a formulation of the variable D corresponds to an isotropic representation.

Table II : Equations of the model

$$\left[\dot{\varepsilon}^{T}\right]=\left[\dot{\varepsilon}^{e}\right]+\left[\dot{\varepsilon}\right]$$

$$\left[\dot{\varepsilon}^{e}\right]=\frac{1+\nu}{E(T)}\left[\dot{\sigma}\right]-\frac{\nu}{E(T)}[\Delta]^{t}[\dot{\sigma}][\Delta]$$

$$\left[\dot{\varepsilon}\right]=\frac{3}{2}\bar{\dot{\varepsilon}}\frac{[\underline{M}][\sigma'-\alpha']}{\overline{\sigma-\alpha}} \text{ with } \bar{\dot{\varepsilon}}=\dot{\varepsilon}_{0}(T,D)\left[\sinh\left(\frac{\overline{\sigma-\alpha}}{N(T,D)}\right)\right]^{n}$$

In these equations : $[\sigma']=[\sigma]-\frac{1}{3}[\Delta]^{t}[\sigma][\Delta]$, $[\alpha']=[\alpha]-\frac{1}{3}[\Delta]^{t}[\alpha][\Delta]$,

$$\overline{\sigma-\alpha}=\left\{\frac{3}{2}[\sigma'-\alpha']^{t}\,[\underline{M}][\sigma'-\alpha']\right\}^{1/2}$$

- Equations of the kinematical hardening variables $[\alpha]$, $[\alpha^{(1)}]$ and $[\alpha^{(2)}]$

$$\left[\dot{\alpha}\right]=p\left(\frac{2}{3}\,Y^{*}(T)\,[\underline{N}][\dot{\varepsilon}]-[\underline{Q}]\left[\alpha-\alpha^{(1)}\right]\bar{\dot{\varepsilon}}\right)-r_{m}(T,D)\sinh\left(\frac{\bar{\alpha}}{\alpha_{0}(T,D)}\right)^{m_{0}}[\underline{N}][\underline{R}]\frac{[\alpha]}{\bar{\alpha}}$$

$$\left[\dot{\alpha}^{(1)}\right]=p_{1}\left(\frac{2}{3}\,Y^{*}(T)\,[\underline{N}][\dot{\varepsilon}]-[\underline{Q}]\left[\alpha^{(1)}-\alpha^{(2)}\right]\bar{\dot{\varepsilon}}\right)$$

$$\left[\dot{\alpha}^{(2)}\right]=p_{2}\left(\frac{2}{3}\,Y^{*}(T)\,[\underline{N}][\dot{\varepsilon}]-[\underline{Q}]\left[\alpha^{(2)}\right]\bar{\dot{\varepsilon}}\right) \text{ with } \left[\dot{\alpha}^{(k)}\right]_{(o)}=0 \text{ and } \bar{\alpha}=\left\{\frac{3}{2}[\alpha]^{t}\,[\underline{R}][\alpha]\right\}^{1/2}$$

- Equations of the scalar variable Y*

$$Y^{*}=Y_{o}(T)+Y$$

$$\dot{Y}=b(Y^{sat}-Y)\bar{\dot{\varepsilon}}$$

- Equation of the irradiation damage variable D

$$\dot{D}=D_{1}(T^{*})(D_{0}(T^{*})-D)\varphi \quad , \quad D(o)=0$$

The integrated form is given by : $D = D_0(T^*)(1 \exp - D_1(T^*)\phi)$.

In these equations, φ is the neutronic flux, ϕ the fluence and T* the irradiation temperature which can be different from the temperature T of the test. The evolution of $D_o(T^*)$ and $D_1(T^*)$ is not specified, these two parameters being considered as constant in the present study.

- Temperature dependence of the parameters

$$E(T) = E_o + E_1 T \qquad \alpha_o(T) = \alpha_1 + \alpha_2 T$$

$$\dot{\varepsilon}_0(T) = \dot{\varepsilon}_1\left(\exp - \frac{\Delta H}{kT}\right)(N(T))^n \qquad r_m(T) = r_{mo}\left(\exp - \frac{\Delta H^*}{kT}\right)(\alpha_o(T))^{m_o}$$

$$N(T) = N_o + N_1 T$$

$$Y_o(T) = Y_1 + Y_2 T$$

- Irradiation dependence of the parameters

$$\dot{\varepsilon}_0(T,D) = \dot{\varepsilon}_0(T)\,(N(T,D))^n \exp\left(-\xi_1 D^{\xi 2}\right) \qquad r_m(T,D) = r_m(T)\exp\left(-\chi_1 D^{\chi 2}\right)$$

$$N(T,D) = N(T) + N_2(1 - \exp - N_3 D) \qquad \alpha_o(T,D) = \alpha_o(T)\exp\left(-\alpha_3 D^{\alpha 4}\right)$$

In this formulation the Voigt matrix notation is adopted :

$[\sigma]^t = [\sigma_{11} = \sigma_1,\ \sigma_{22} = \sigma_2,\ \sigma_{33} = \sigma_3,\ \sigma_{12} = \sigma_4,\ \sigma_{13} = \sigma_5,\ \sigma_{23} = \sigma_6]$

$[\varepsilon]^t = [\varepsilon_{11} = \varepsilon_1,\ \varepsilon_{22} = \varepsilon_2,\ \varepsilon_{33} = \varepsilon_3,\ 2\varepsilon_{12} = \varepsilon_4,\ 2\varepsilon_{13} = \varepsilon_5,\ 2\varepsilon_{23} = \varepsilon_6]$

$[\Delta]^t = [1, 1, 1, 0, 0, 0]$

[M], [N], [Q], [R] have an orthotropic symmetry. For example for [M] :

$$[\underline{M}] = \begin{bmatrix} M_{11} & M_{12} & M_{13} & & & \\ M_{13} & M_{22} & M_{23} & & & \\ M_{13} & M_{23} & M_{33} & & 0 & \\ & & & M_{44} & & \\ & 0 & & & M_{55} & \\ & & & & & M_{66} \end{bmatrix}$$

with the incompressibility relations :

$$M_{11} + M_{12} + M_{13} = 0$$

$$M_{13} + M_{22} + M_{23} = 0$$

$$M_{13} + M_{23} + M_{33} = 0$$

IV - IDENTIFICATION OF THE MODEL AND SIMULATIONS

The parameters of the model are obtained by numerical simulations on uni and biaxial tensile and creep tests at 350 and 400°C. The evolutions of parameters with the temperature are verified by comparing simulations with tests results at 380°C. On Fig. 1 the model is in good agreement with biaxial tensile tests performed at 350°C with different ratios α. Thus the description of the anisotropy of the tube is correct. The same adequation between tests and predictions has been obtained for three complex loadings realized at 350, 380 and 400°C, Fig. 4, which are representative of a PCI transient : biaxial tensile test, α = 0.5, with an imposed hoop strain rate of $2\ 10^{-5} s^{-1}$ followed by a relaxation test. The Fig. 5 illustrates the capability of the model to simulate biaxial tensile tests at 350°C for different fluences. The results are fairly good. In the same way, the Fig. 6 and 7 show that the model is able to predict the mechanical behavior of irradiated cladding tubes at 350 and 380°C.

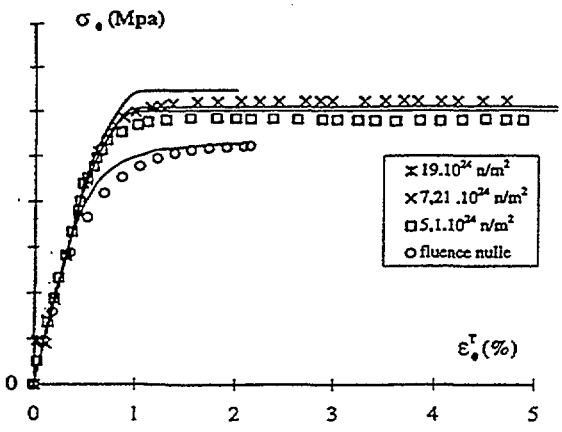

• Fig. 6 : Modeling of a tensile-internal pressure test for different strain rates at 380°C, performed on irradiated cladding tubes until 4 cycles in PWR (Program C).

• Fig. 5 : Biaxial tensile tests performed at 350°C for an imposed hoop strain rate of $2.^{10-4}s^{-1}$ for different fluences. Experimental results and simulations.

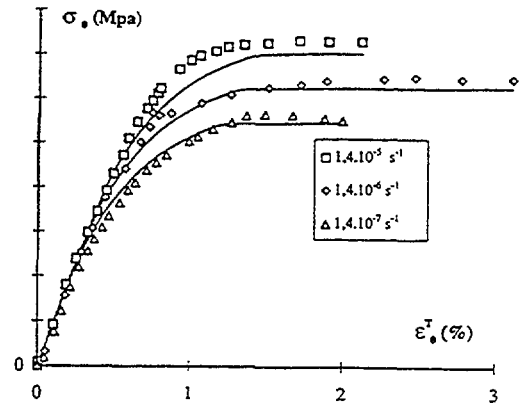

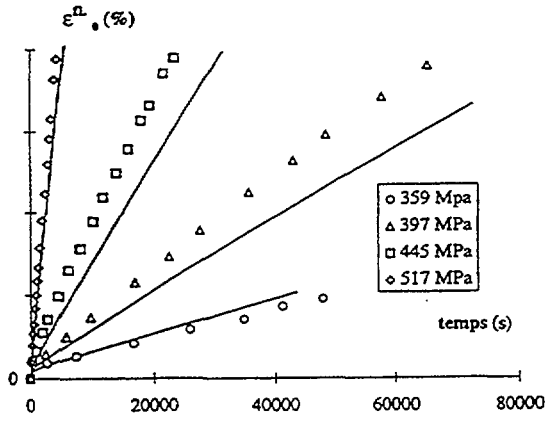

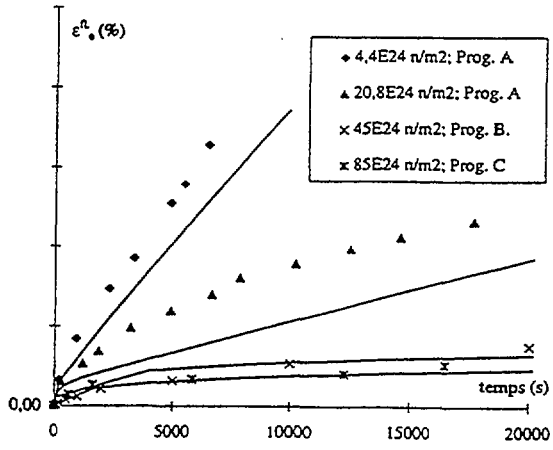

• Fig. 7 : Simulation of tensile-internal pressure tests performed at 350°C on irradiated cladding tubes :
  - a - irradiated 1000 H, for different stress levels
  - b - $\sigma_{\theta\theta} = 415$ MPa, for different fluences (Programs A,B,C).

V - CONCLUSIONS

The analysis of the out-of-flux experimental data basis composed of biaxial tensile, creep and relaxation tests carried out on irradiated CWSR cladding tubes shows the hardening and a decrease in creep deformation due to neutron irradiation. These irradiation effects are introduced into this model through an internal state variable of damage which is a function of the fluence. Finally, we show the ability of the modeling to calculate the anisotropic behavior of cladding tubes during tensile, high hoop stress levels creep and relaxation tests in the temperature range 350-400°C and fluences range 0-85.10^{24} n/m^2 (E > 1 MeV). This model is already introduced in the EDF finite element Code-Aster and will be implemented in the cladding tube calculation code of EDF, Cyrano 3 to allow the calculation of PCI transients.

ACKNOWLEDGEMENTS

The authors want to thank their industrial partners for financial and technical supports in the R & D programs used to develop this model. In particularly, we would like to thank Framatome Nuclear Fuel for supplying the material on which that study has been conducted, Atomic Energy Commission for having carried out the experimental tests on irradiated materials, as well EDF/SEPTEN for its financial support of this work.

REFERENCES

1. Baron, D. and Bouffioux, P. 1989. Le crayon combustible des réacteurs à eau pressurisée de grande puissance. *Rapport EDF HT.MZ/88-27A*

2. Beauregard, R.J., Clevinger, J.S. & Murty, K.L. 1977. Effect of annealing temperature on the mechanical properties of Zircaloy-4 cladding. *Proc. SMIRT IV, paper C3/5*

3. Murty, K.L. 1989. Applications of crystallographic textures of Zirconium alloys in nuclear industry. *Proc. Zirc. in the Nucl. Ind., Symp. VIII, ASTM STP 1023, 570*

4. CEA, Framatome & EDF Cooperative program. 1995. *Propriétary data.*

5. CEA, Framatome & EDF Cooperative program. 1995. *Propriétary data.*

6. Bernaudat, C. 1995. EDF/SEPTEN. *Personnal communication.*

7. Epri, B. & W. 1983. *Cooperative Program on PWR Fuel Rod Performance NP 2848, Project 711-1*

8. Higgy, R. & Hammad, F.H. 1972. Effect of neutron irradiation on the tensile properties of Zircaloy-2 and Zircaloy-4. *J. Nucl. Mat.*, 44, 215-277

9. Franklin, D.G. 1982. Zircaloy-4 cladding deformation during power reactor irradiation. *V ASTM STP,* 754, 235-267

10. Franklin, D.G., Lucas, G.E. & Bement, A.L. 1983. Creep of Zirconium alloys in nuclear reactors. *ASTM, Special Techn. Publ. 815,* code 04-81 5000-35

11. Baty, D.L., Pavinich, W.A., Dietrich, M.R., Clevinger, G.S. & Papazoglou, T.P. 1984. Deformation characteristics of cold-worked and recristallized Zircaloy-4 cladding. *VI Int. Symp. on Zirconium in the Nuclear Industry,* ASTM-STP 824, 306-339

12. Delobelle, P. 1993. Synthesis of the elastoviscoplastic behavior and modelization of an austenitic stainless steel over a large temperature range under uni and biaxial loadings. Int. J. Plast., *9, 87-118*

13. Delobelle, P., Robinet, P., Geyer, P., Bouffioux, P. & Le Pichon, I. 1995. A unified model to describe the anisotropic viscoplastic behavior of Zircaloy-4 tubes. *11th Int. Symp. ASTM-STP*, 1295, 373-393